**SANDIA REPORT**
SAND2007-8095
Unlimited Release
Printed January 2008

# Final Report on LDRD Project 105967: Exploring the Increase in GaAs Photodiode Responsivity with Increased Neutron Fluence

Ethan L. Blansett, Darwin K. Serkland, Michael J. Cich, Kent M. Geib,
Gregory M. Peake, Robert M. Fleming, Diana L. Wrobel, Theodore F. Wrobel

Prepared by
Sandia National Laboratories
Albuquerque, New Mexico 87185 and Livermore, California 94550

Sandia is a multiprogram laboratory operated by Sandia Corporation,
a Lockheed Martin Company, for the United States Department of Energy's
National Nuclear Security Administration under Contract DE-AC04-94AL85000.



Issued by Sandia National Laboratories, operated for the United States Department of Energy by Sandia Corporation.



Available to DOE and DOE contractors from
U.S. Department of Energy
Office of Scientific and Technical Information
P.O. Box 62
Oak Ridge, TN 37831

Telephone: (865) 576-8401
Facsimile: (865) 576-5728
E-Mail: reports@adonis.osti.gov
Online ordering: http://www.osti.gov/bridge

Available to the public from
U.S. Department of Commerce
National Technical Information Service
5285 Port Royal Rd.
Springfield, VA 22161

Telephone: (800) 553-6847
Facsimile: (703) 605-6900
E-Mail: orders@ntis.fedworld.gov
Online order: http://www.ntis.gov/help/ordermethods.asp?loc=7-4-0#online

SAND2007-8095
Unlimited Release
Printed January 2008

# Final Report on LDRD Project 105967: Exploring the Increase in GaAs Photodiode Responsivity with Increased Neutron Fluence

Ethan L. Blansett, Darwin K. Serkland, Michael J. Cich, Kent M. Geib, Gregory M. Peake, Robert M. Fleming, Diana L. Wrobel, Theodore F. Wrobel

Sandia National Laboratories
P. O. Box 5800
Albuquerque, New Mexico 87185-MS 1167

## Abstract

A previous LDRD studying radiation hardened optoelectronic components for space-based applications led to the result that increased neutron irradiation from a fast-burst reactor caused increased responsivity in GaAs photodiodes up to a total fluence of $4.4x10^{13}$ neutrons/$cm^2$ (1 MeV Eq., Si). The silicon photodiodes experienced significant degradation. Scientific literature shows that neutrons can both cause defects as well as potentially remove defects in an annealing-like process in GaAs. Though there has been some modeling that suggests how fabrication and radiation-induced defects can migrate to surfaces and interfaces in GaAs and lead to an ordering effect, it is important to consider how these processes affect the performance of devices, such as the basic GaAs p-i-n photodiode. In this LDRD, we manufactured GaAs photodiodes at the MESA facility, irradiated them with electrons and neutrons at the White Sands Missile Range Linac and Fast Burst Reactor, and performed measurements to show the effect of irradiation on dark current, responsivity and high-speed bandwidth.

## Acknowledgments

We thank Victoria Montano for fabricating the GaAs photodiodes in the MESA microfab cleanroom. We thank Gordon A. Keeler for initially setting up the two single-frequency lasers for photodiode bandwidth measurements. Sandia is a multiprogram laboratory operated by Sandia Corporation, a Lockheed Martin Company, for the United States Department of Energy's National Nuclear Security Administration under contract DE-AC04-94AL85000.

# Contents

**(This page is left blank intentionally.)**

# 1. Introduction

## 1.1. LDRD Project Overview

In a previous LDRD study, GaAs photodiodes and vertical-cavity surface-emitting lasers (VCSELs) were tested with both proton and neutron radiation to determine their usefulness in space applications [1]. Neutron radiation measurements were performed with a fast-burst reactor at the Army Pulse Radiation Facility located on Aberdeen Proving Ground in Maryland. Devices measured included four GaAs photodiodes that were attached to a circuit board and provided by Peregrine Semiconductor. Two of the GaAs photodiodes were manufactured by EMCORE (GaAsPD1,2) and two we believe were manufactured by AXT (GaAsPD3,4). We also irradiated silicon photodiodes (EGG&G FND100), and GaAs VCSELs that were attached above silicon photodiodes. The silicon photodiodes were reverse biased at 10 V and the GaAs photodiodes were reverse biased at 1 V.

After irradiation, the photodiodes were placed into a test station consisting of an 850 nm VCSEL and a coupling lens that experienced no radiation. The response of these photodiodes as well as that of a reference silicon photodiode that was not irradiated was measured. The response of the VCSEL-Si photodiode pairs were also measured, though in this case, the degradation of the VCSEL alone must be determine by comparing to the degradation of the pair to the degradation of the individual Si photodiodes. The response for each detector or VCSEL-detector pair with increased accumulated fluence (1 MeV eq., Si) is shown in Figure 1.1. The response is normalized to the response before irradiation.

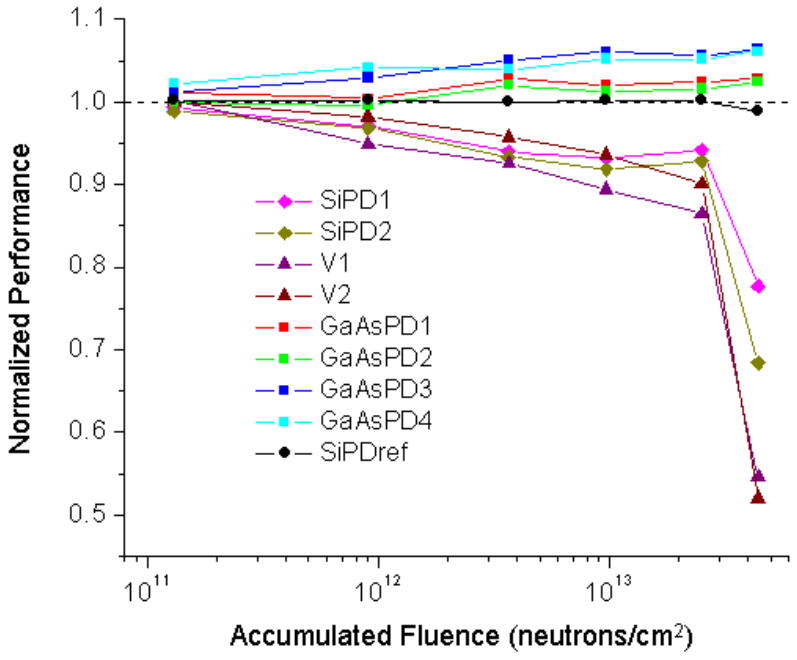


**Figure 1.1. Normalized performance of two Si photodiodes (SiPD1,2), two VCSELs coupled into Si photodiodes (V1,2), four GaAs photodiodes (GaAsPD1-4) and a reference Si photodiode that was not irradiated (SiPDref). The fluence levels are 1 MeV equivalent silicon levels.**

The silicon photodiodes as well as the VCSEL-silicon photodiode pair show clear degradation with increasing neutron fluence, especially above $2x10^{12}$ neutrons/cm$^2$ (1 MeV Eq., Si). The GaAs detectors, however, show an increase in responsivity with increasing fluence. Since the Si photodiodes experienced a roughly 30% degradation and the VCSEL-Si photodiode pair experienced a roughly 50% degradation at the highest fluence level, we can deduce that the VCSEL experienced a roughly 30% decrease in output power. After the total fluence of $4.4x10^{13}$ neutrons/cm$^2$, the silicon photodiodes had a leakage current of about 2 A (compared to a signal of about 400 A with laser on) and the GaAs photodiodes had a leakage current less than 1 pA (compared to a signal of about 30 A with laser on). The leakage current of the GaAs photodiodes was clearly too small to explain the increase in current measured with increased radiation.

The response of the GaAs photodiodes is intriguing. Though the level of increase in responsivity is modest, the fact that it is increasing at all is an interesting result. There also appears to be a small difference between the photodiodes obtained from different vendors, though it is the dramatic difference in behavior compared to the Si photodiodes and GaAs emitters (VCSELs) that demands explanation. To gain further insight into the radiation response of these detectors and emitters, it is useful to know how they respond to proton irradiation.

For the proton measurements, coupled VCSEL-detector pairs were irradiated with 63 MeV protons at the Crocker Nuclear Laboratory at University of California, Davis. The GaAs photodiodes, nominally identical to the four irradiated with neutrons, were also attached to a circuit board with traces and a ribbon connector. We attached VCSELs above silicon photodiodes (EG&G FND100) to obtain a comparison between Si and GaAs photodiodes. At a total fluence level of $5x10^{13}$ protons/cm$^2$, the VCSEL-detector pairs labeled GaAs1 and 2 experienced about 45% decrease in signal, GaAs3 and 4 experienced a 55% reduction in signal, and Si1 and 2 experienced a 75% reduction in signal.

From comparing the neutron and proton irradiation results, it is clear that the increase in responsivity of the GaAs photodiodes is unique to the neutron irradiation. The main difference between neutron and proton radiation in general is that the protons cause ionization in addition to displacement damage, whereas the neutron has no charge with which to cause direct ionization. In addition, though both particles can cause defects through interactions with the target atomic nuclei, the types of nuclear interactions and the cross sections are different. To test whether it is the ionization that causes the degradation seen with protons, irradiation with only gamma rays should be performed, since they cause ionization but no displacement damage.

In an attempt to understand the behavior of the GaAs photodiodes to neutron radiation, a literature search has been performed. There have been studies of the effects of radiation on GaAs material scattered throughout the last forty years. In the 1960s, the effect of neutron irradiation on GaAs was first discussed, with some results showing an increase in the absorption coefficient in GaAs at photon energies within the bandgap [2]. By the early 1990s, it was discovered that some of the electronic properties of GaAs may improve due to neutron irradiation at low fluence levels, with degradation occurring at higher levels [3].

It has been proposed that there is a radiation-induced order effect in GaAs, similar to the effect that thermal annealing can have on defects [4]. One model has suggested that recombination centers can be reduced by a migration of defects originally in the material as well as radiation-induced defects to surfaces, phase boundaries or interfaces [5]. The details of this process do not seem to be well-understood, and have not been subjected to sufficient experimental verification. This project was an attempt to understand in more detail how neutron and electron irradiation affect the device properties of GaAs photodiodes, such as dark current, responsivity and high-speed bandwidth.

## 1.2. Technical Problem and Approach

To further investigate the effect of radiation on GaAs photodiodes, the devices were fabricated at Sandia National Laboratories at the MESA facility in order to control and understand the details of the device composition and material properties. Previous work has compared the effects of electron and neutron irradiation on basic device properties such as carrier mobility [4]. We decided to also perform electron and neutron irradiation in the hope that comparisons could be made between our photodiode dark current, responsivity and bandwidth measurements and the previous bulk device properties such as carrier mobility and photoluminescence spectra. The electron irradiation would also add to the knowledge gained through previous proton and neutron irradiation measurements made at Sandia. Details of the photodiode fabrication, irradiation, and subsequent measurements are given in later sections.

# 2. GaAs PIN Photodiodes

## 2.1. Photodiode Structure

The GaAs PIN photodiodes fabricated for this project were based on a Sandia radiation hardened design reported by Wiczer, et al., in 1984.[6,7] Figure 2.1 shows a cross-sectional schematic of the photodiode device structure. The key feature of this structure is the incorporation of a higher bandgap n-type “cladding” layer, of composition $Al._3Ga._7As$, between the GaAs absorption layer and the substrate, which prevents radiation induced holes generated in the substrate from diffusing to the active region, where they would be swept to the p-side of the junction and result in radiation induced photocurrent.

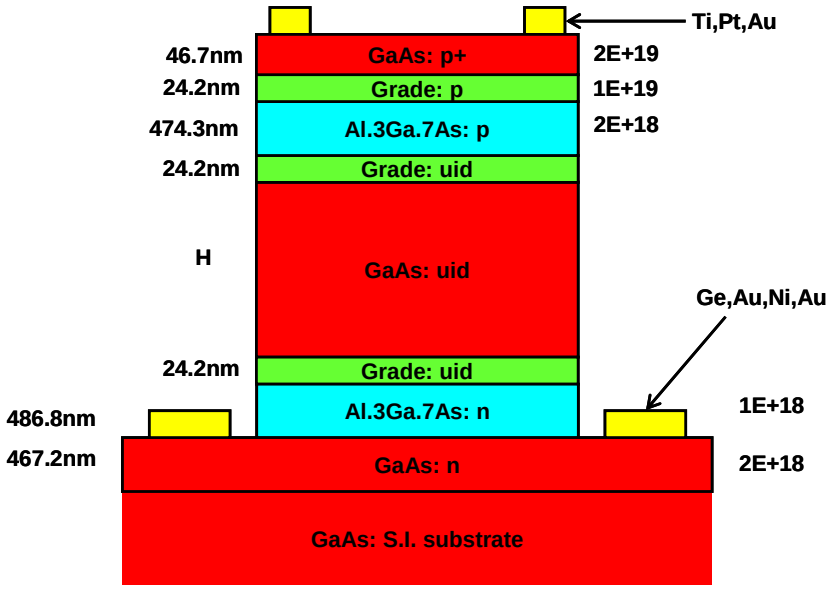


**Figure 2.1. Cross-sectional schematic of rad-hard GaAs PIN photodiode. The thickness of each layer is noted on the left side and the doping level is noted on the right side. The abbreviation uid = un-intentionally doped. "Grade" denotes a linear compositional grade between the compositions of the two adjacent layers. Two photodiode wafers were grown, each with a different GaAs absorbing layer thickness H: wafer EMC8307 (H=911.1nm) and wafer EMC8308 (H=1845.5nm).**

Two photodiode wafers, differing in the thickness of the GaAs absorption layer, were grown by MOCVD for this project. The first wafer EMC8307 had a GaAs layer thickness H = 911.1nm, and the second wafer EMC8308 had a GaAs layer thickness H = 1845.5nm. For simplicity, we often refer to EMC8307 as a 1-um photodiode and EMC8308 as a 2-um photodiode, in order to indicate the approximate thickness of the "intrinsic" un-intentionally doped region.

Figure 2.2 shows a partially fabricated photodiode being illuminated with an 850-nm laser spot in the middle of the aperture. The top p-type anode contact metal is a 10-um wide annulus whose inner diameter serves as the aperture of the photodiode. The photodiode shown in Figure 2.2 has a 70-um aperture, whereas most of the high-speed photodiodes that were irradiated for this project had 60-um apertures. A top mesa, having a nominal radius 2um larger than the outer radius of the top metal, is etched through the p-type and intrinsic layers, stopping in the n-type cladding layer. A lower n-type cathode contact metal annulus is deposited around the base of the mesa. Finally, a lower "isolation" mesa is etched outside the outer diameter of the cathode metal to electrically isolate each photodiode from its neighbors on the substrate. After these steps are completed, the photodiode is functional and ready for preliminary electrical and optical testing, as indicated by the wafer probes and incident laser beam in Figure 2.2.

**Figure 2.2. Top view microscope photograph of a partially fabricated photodiode being illuminated with an 850-nm laser spot inside the 70-um top metal aperture.**

To finish the photodiode fabrication we applied Ti/Au bond pads, as shown by the green regions in the mask layout of Figure 2.3. Note that the anode and cathode bond pads lie on a 125-um center-to-center pitch in the x direction. Finally, we deposited a quarter-wave (at 850nm) layer of SiN (n=1.97) by PECVD to serve as an anti-reflection coating.

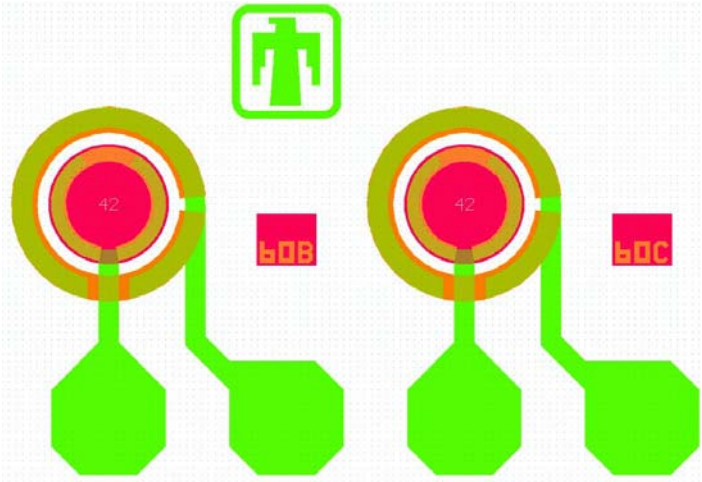


**Figure 2.3. Mask layout of two adjacent 60-um-aperture photodiodes. Bond pad metal is shown in green.**

## 2.2. Photodiode measurements

After fabrication and dicing, we measured (without illumination) forward voltage versus current (VI) and dark current versus reverse bias voltage (IV). The forward VI measurement was done using a 4-point Kelvin contact configuration, as shown in Figure 2.4. Typical VI measurement data are shown in Figure 2.5. The VI measurements are useful for determining the series resistance of the photodiode, due to the ohmic contact resistance, doped layer resistance, and spreading resistance from the annular contacts. A

series resistance of 50 Ohms will cut in half the bandwidth (and amplitude) measured into a 50-Ohm load resistance. The data shown in Figure 2.5 correspond to a series resistance of 13 Ohms at a forward bias current of 4.5 mA.

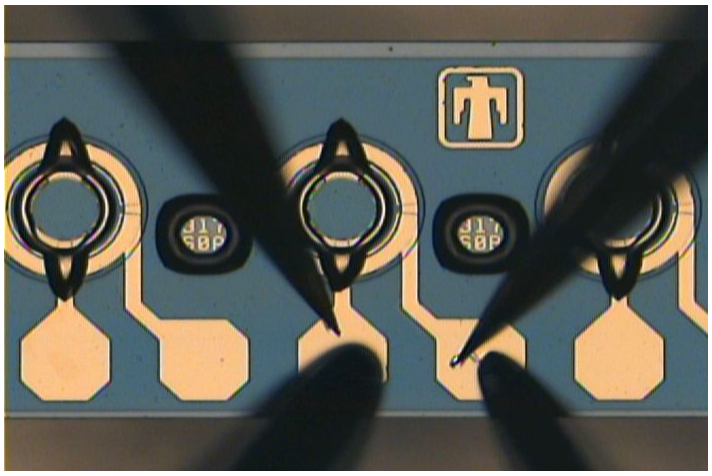

**Figure 2.4. Top view of 4-point voltage versus current (VI) measurement.**

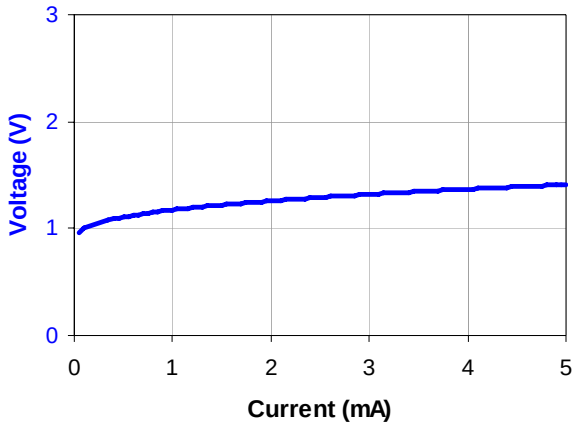


**Figure 2.5. Forward voltage versus current (VI) measurement on photodiode EMC8308-B die 366 device 60BT before irradiation.**

Dark current was measured accurately with a simple 2-point contact configuration. Dark current versus reverse bias voltage (IV) data are shown in Figure 2.6 for a 60-um-aperture photodiode, nominally identical to the ones that were irradiated. The dark current shown in Figure 2.6 is 7.7 pA at a reverse bias voltage of 2 V.

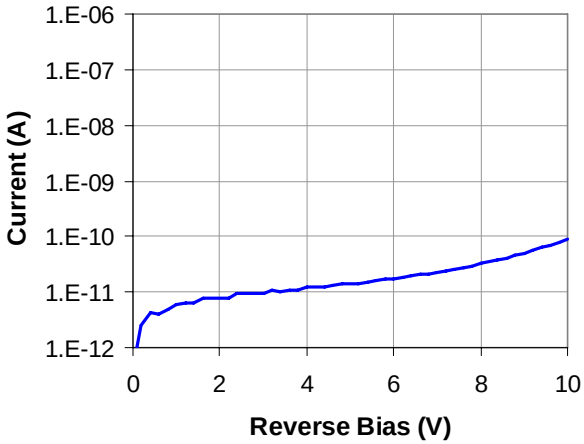


**Figure 2.6. Dark current versus reverse bias voltage measurement on photodiode EMC8308-B die 317 device 60BT before irradiation.**

# 3. Irradiation results

## 3.1. Radiation exposures

After being pre-tested, the GaAs photodiode chips were mounted in die form into 1-inch square clear plastic boxes for irradiation. The table in Figure 3.1 shows the planned irradiation conditions for each plastic box, and the contents of each box; either one GaAs chip or four GaAs chips per box. At a minimum, one linear array of 60-um-aperture photodiodes from wafer EMC8308-B was placed in each plastic box. Each linear array contained either five (60A, 60B, 60C, 60D, 60E) or three (60F, 60G, 60H) photodiodes, of which the second photodiode (60B or 60G) in each array was pre-tested.

| Box Number | Radiation Type | Fluence cm^-2 | 8308-B 60um | 8308-B variable | 8308-B 500um | 8307-A 60um |
|---|---|---|---|---|---|---|
| 01 | neutron | 1E+12 | 364_60GT | | | |
| 02 | neutron | 1E+13 | 364_60BT | 364_VV | 363_500 | 367_60GT |
| 03 | neutron | 1E+14 | 366_60BT | 366_VV | 365_500 | 368_60GT |
| 04 | neutron | 1E+15 | 366_60GT | | | |
| 05 | electron | 1E+12 | 365_60BT | | | |
| 06 | electron | 3E+12 | 314_60BT | | | |
| 07 | electron | 1E+13 | 314_60GT | 314_VV | 313_500 | 317_60GT |
| 08 | electron | 3E+13 | 316_60GT | | | |
| 09 | electron | 1E+14 | 316_60BT | 316_VV | 315_500 | 318_60GT |
| 10 | electron | 3E+14 | 315_60BT | | | |
| 11 | electron | 1E+15 | 315_60GT | | | |
| 12 | -- | -- | | | | |

**Figure 3.1. Table of irradiation fluence levels and contents of each 1-inch square plastic box.**

Inside each clear plastic box, a thin sheet of tacky blue tape was stretched over a 0.75-inch square of electrically conductive plastic (cut from a waffle pack lid). The GaAs chips were placed onto the surface of the tacky blue tape, in either the upper right or upper left corner of the box, as shown in Figure 3.2(a). This placement of device chips allowed four plastic boxes to be tiled such that the devices in the four boxes all fit within a 1-inch diameter electron radiation beam, as shown in Figure 3.2(b).

(a) 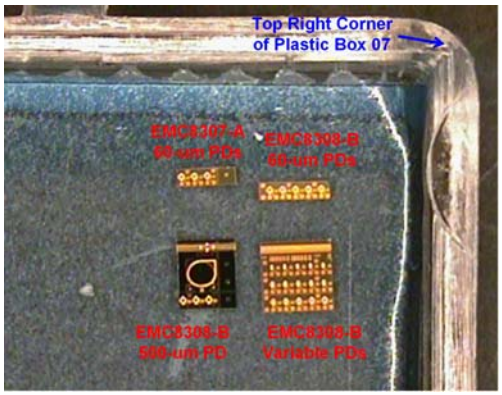

(b) 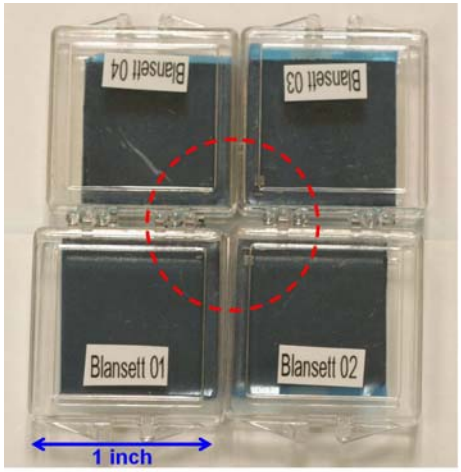


**Figure 3.2. (a) Picture of four photodiode chips positioned in the upper right corner of box number 07. (b) Picture of four plastic boxes tiled to fit all photodiode chips within a 1-inch diameter electron beam (indicated by the red dashed circle).**

## 3.2. Dark current measurements

Figure 3.3 shows the measured dark current versus reverse bias voltage (IV) measurements on four 60-um-diameter-aperture photodiodes subjected to different neutron fluence levels. These photodiodes (from wafer EMC8308-B) all had 2-um thick intrinsic regions. As reported in other publications, the dark current increases with fluence level.

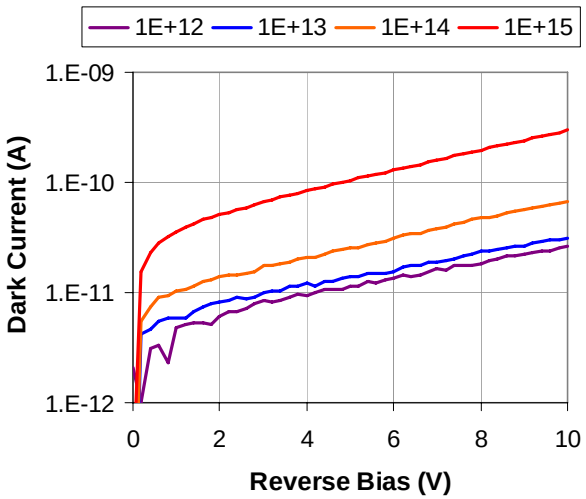


**Figure 3.3. Measured dark current versus reverse bias voltage (IV) of four 60-um-aperture photodiodes subjected to different fluence levels of neutron radiation. The legend shows the fluence level in units of neutrons/cm$^2$.**

We quantify the radiation-induced damage effect on dark current according to the equation

$$I_D(\Phi) = I_D(0) + K_D\Phi,$$

where $I_D(\Phi)$ is the dark current measured after irradiation at fluence level $\Phi$, $I_D(0)$ is the dark current before irradiation, and $K_D$ is the damage factor for dark current. Figure 3.4 shows the dark current measured at 5V reverse bias versus neutron fluence. A linear fit yields a neutron radiation damage coefficient $K_D$ = 9E-26 A cm$^2$. Given that these 60-um-aperture photodiodes have a mesa diameter of 84 um, the diode area is 5.54E-5 cm$^2$. Thus, we calculate a dark current density damage coefficient $K_{JD} = K_D/A$ = 1.6E-21 A.

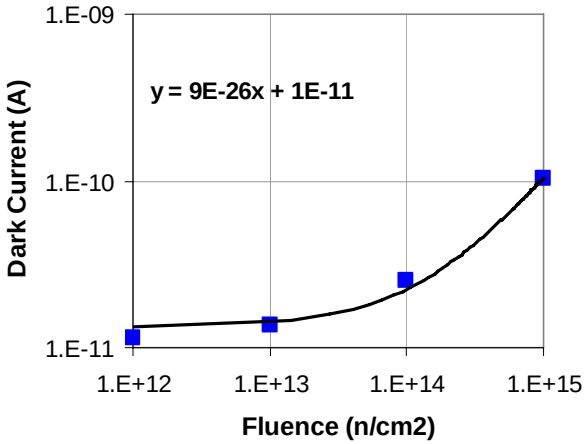


**Figure 3.4. Measured dark current at 5-V reverse bias versus neutron fluence level. A linear fit to the four data points is also shown.**

Though it seems intuitive that the dark current would increase with increased neutron fluence, results from measurements on photoconductive semiconductor switch (PCSS) devices indicate that increasing damage leads to a reduction in dark current. The difference between these devices is interesting and relates to the characteristic electronic transport length and time scales as compared to device dimensions.

The dark current - the current that a p-n junction passes under reverse bias - has several contributors depending on the semiconductor physical properties (e.g. bandgap) and junction design (e.g. doping levels, surface passivation). For both the PCSS and photodetectors, the surface can be neglected because the perimeter of the device is small relative to the area. In the case of GaAs (for both devices), the band-to-band thermal excitation rate at room temperature is negligible. This leaves as the primary source of dark current the thermal excitation of carriers out of deep levels (associated with lattice defects) into the conduction or valence bands. For simplicity, we will examine the particular case of a deep donor with a energy level in the bandgap that is below the Fermi level in equilibrium. This means the defect has two charge states - zero and plus one - depending on whether or not it has trapped an electron. Because the equilibrium Fermi level is above the defect level, the defect usually is in the neutral state (has trapped an electron) The model is that an electron trapped at the deep donor will occasionally acquire enough thermal energy to be promoted to the conduction band, leaving a positively charged defect behind. This defect will subsequently return to its equilibrium state, either by capturing an electron from the conduction band, or by emitting a hole to the valence band.

The other three cases (deep donors above the Fermi level, deep acceptors above and below the Fermi level) have analogous behavior, capturing or emitting holes or electrons to move between two charge states. The timescale for a carrier to be generated or trapped by this non-radiative generation/recombination process is called the Shockley-Read-Hall (SRH) lifetime. For pure (non-damaged) GaAs it is ~ 1 ns. Lattice damage shortens this timescale, down to the few picosecond level for heavily damaged GaAs. Some growth methods for GaAs can produce material SRH lifetimes as small as ~100 fs.

Both the PCSS and photodiodes accumulate more lattice defects under irradiation. So why shouldn't the dark current be increased in both devices, since there are more defects to generate more current in both cases? They both operate at about the same electric field (~2 V/micron), have essentially intrinsic material (carrier concentration ~$10^7/cm^3$ ) in the active region?

The difference has to do with the distance a carrier has to travel to reach the anode or cathode to appear at the external circuit. In the case of a photodiode, the distance a carrier has to travel to reach the anode or cathode (whether it be optically-generated detector current or thermally-generated dark current) is on the order of 1 micron. This distance is traveled in about 1-2 ps at these electric fields (2V/micron). (Calculate this from F=qE, F=ma, and $d=0.5*a*t^2$) Note that this corresponds to an average carrier velocity of ~ $10^8$ cm/s which is higher than the typical saturated velocity of ~1e7 cm/s. For the saturated carrier velocity to apply, the carrier must undergo at least a few scattering events before reaching the cathode. The mean scattering time for a carrier in GaAs is on the order of a

few picoseconds, longer than the time it takes to reach the anode or cathode, so that the ballistic velocity is more appropriate than the saturated velocity. Each time a lattice defect thermally emits a carrier, that carrier quickly reaches the device contacts and contributes to the dark current. The carrier mobility does not come into the equation because the transport is ballistic.

On the other hand, the PCSS device dimensions are such that the carrier has to travel ~100 microns to reach the anode or cathode. Over this distance any generated (excess) carrier will undergo many scattering events, so the carrier velocity is the saturation velocity. Then it would take ~ 1 ns for the carrier to reach the anode or cathode. However, this travel time is longer than the SRH lifetime. Then a generated carrier is more likely to be retrapped at a lattice defect than it is to reach the device contacts. Therefore the increased defect concentration after irradiation, though it increases the total thermal generation rate, also acts to trap any thermally generated carriers before they can reach the device contacts. In effect, each carrier runs into many stoplights on its path where it has to wait to be re-emitted to continue its journey. Thus the irradiation actually reduces the overall current compared to the un-irradiated case.

## 3.3. Responsivity measurements

We measured the responsivity (photodiode output current divided by incident optical power) of several photodiodes subjected to neutron or electron radiation at various fluence levels. Figure 3.5(a) shows a 60-um-diameter-aperture photodiode being illuminated by a laser at 850-nm, the standard wavelength for short-distance data communications. We note that the dominant commercial use of GaAs PIN photodiodes is in fiber-optic receivers for short distance (<300m) data communication links, using 850-nm vertical-cavity surface-emitting lasers (VCSELs), operating at data rates from 1 to 10 Gbit/s. Figure 3.5(b) shows a schematic diagram of the optical setup for measuring responsivity. A beam splitter (BS) taps approximately 4% of the incident 850-nm laser beam to measure incident power with a monitor detector (Dmon) during the measurement. The incident power is calibrated (relative to the measured monitor signal) using a New Focus model 2031 silicon detector (Dcal) with a published responsivity of 0.58 ± 0.03 A/W at 850nm. The incident beam is focused to a diameter smaller than 60 um, using a Thorlabs model A397TM-B aspheric lens (L3, f=11.0mm) that is anti-reflection coated from 600 to 1050nm.

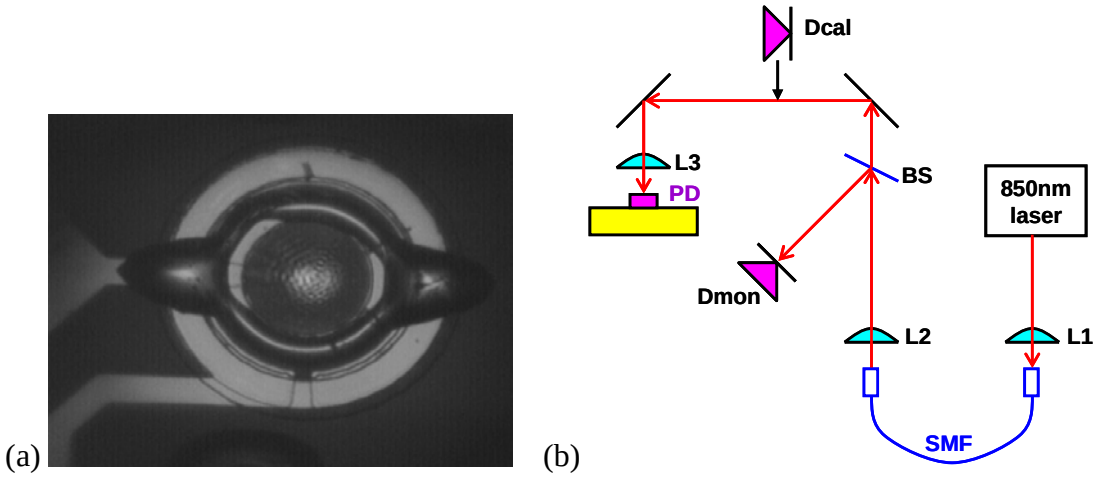


**Figure 3.5. (a) Picture of 60-um-aperture photodiode illuminated at 850 nm for responsivity measurement. (b) Schematic diagram of responsivity measurement setup. A beamsplitter (BS) taps 4% of the beam power to a monitor photodetector (Dmon) as a means of measuring the incident power at all times. The 850-nm laser beam is focused entirely within the photodiode (PD) aperture with lens L3.**

Figure 3.6 shows the responsivity of four neutron-irradiated photodiodes. These photodiodes (from wafer EMC8308-B) all had 2-um thick intrinsic regions. There was no discernable damage at fluence levels below $1x10^{13}$ neutrons/cm$^2$. At the highest fluence, $1x10^{15}$ neutrons/cm$^2$, the responsivity at 0 V bias was reduced by 13%. However, at higher reverse bias voltages (> 2 V), the responsivity was only slightly degraded (< 4%).

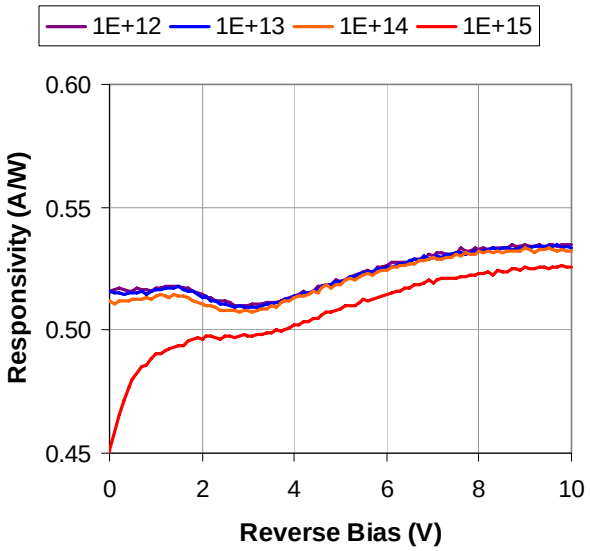


**Figure 3.6. Measured responsivity versus reverse bias voltage of four 60-um-aperture photodiodes subjected to different fluence levels of neutron radiation. The legend shows the fluence level in units of neutrons/cm$^2$.**

The physical explanation for the reduced responsivity after irradiation is electron-hole recombination at radiation-induced defect sites due to Shockley-Read-Hall (SRH) recombination. Quantitatively, the effect of radiation damage on minority carrier recombination lifetime $\tau$ is expressed by

$$\tau^{-1}(\Phi) = \tau^{-1}(0) + K_{\tau}\Phi ,$$

where $\tau(\Phi)$ is the lifetime after irradiation at fluence level $\Phi$, $\tau(0)$ is the lifetime before irradiation, and $K_\tau$ is the minority carrier lifetime damage coefficient. Thus, the minority carrier recombination rate $\gamma=1/\tau$ increases linearly with fluence (damage). When a photon is absorbed in the intrinsic region of the photodiode, it produces an electron-hole pair. If those minority carriers are swept from the depletion region before they recombine, then they contribute to the measured photocurrent (or responsivity). As the reverse bias voltage increases, the electric field in the depletion region increases and thus the carriers are swept out more rapidly. For GaAs, the drift velocity saturates at $1x10^7$ cm/s at fields above approximately 10 kV/cm. For reference, at a reverse bias voltage of $V_R$ = 2 V, the electric field across the 2-um intrinsic region is approximately 16 kV/cm = $(V_R + V_{bi})/2um$, where $V_{bi}$ is the "built-in" voltage of 1.2V. Thus, if the average carrier travels 1um (half of the intrinsic region thickness) at the saturated drift velocity of 0.1um/ps, the average transit time is $t_{tr}$ = 10ps. At a reverse bias of 2 V, the responsivity of the photodiode irradiated at $1x10^{15}$ neutrons/cm$^2$ was reduced 3.3% (from 0.513 to 0.497 A/W). Thus, we estimate that $t_{tr}/\tau(\Phi)$ = 3.3%, so the minority carrier lifetime is reduced to $\tau(\Phi)$ = 302 ps after irradiation at a fluence of $1x10^{15}$ neutrons/cm$^2$. Hence, we determine a minority carrier lifetime damage coefficient of $K_\tau = 3.3 \times 10^{-6}$ s$^{-1}$ / (n/cm$^2$).

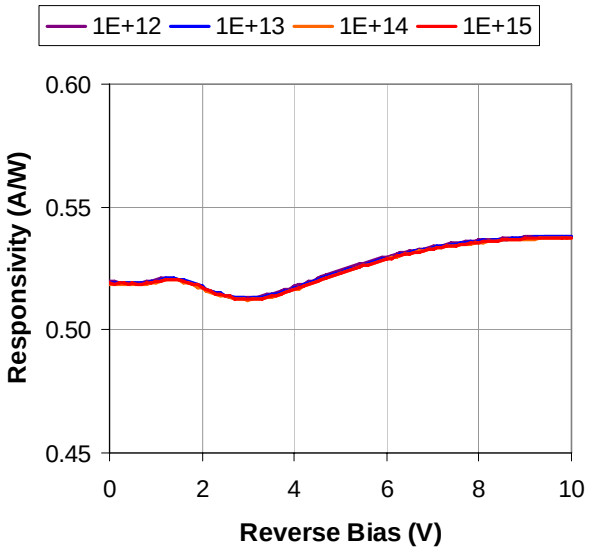


**Figure 3.7. Measured responsivity versus reverse bias voltage of four 60-um-aperture photodiodes subjected to different fluence levels of electron radiation. The legend shows the fluence level in units of electrons/cm$^2$.**

Finally, Figure 3.7 shows the responsivity of four electron-irradiated photodiodes. These photodiodes (from wafer EMC8308-B) all had 2-um thick intrinsic regions. There was no discernable damage over the range of fluence levels tested from $1x10^{12}$ to $1x10^{15}$ electrons/cm$^2$. Thus we conclude that electrons are less effective than neutrons at creating lattice damage (defects) in GaAs.

## 3.4. Bandwidth measurements

We measured the frequency response (AC photocurrent output versus frequency of input optical modulation) of several photodiodes subjected to neutron radiation at various fluence levels. **Error! Reference source not found.**(a) shows a 60-um-diameter-aperture photodiode, illuminated by two lasers at 850-nm and electrically contacted with a 40-GHz coplanar probe (Cascade Microtech model ACP-40_GSG125). **Error! Reference source not found.**(b) shows a schematic diagram of the setup for measuring photodiode bandwidth. The outputs of two 850-nm single-frequency tunable lasers are combined with a 50% beam splitter (BS1) and coupled into a single-mode fiber (SMF). The fiber output beam is focused to a diameter smaller than 60 um, using a Thorlabs model A397TM-B aspheric lens (L3, f=11.0mm) that is anti-reflection coated from 600 to 1050nm. A coplanar probe contacts the photodiode and provides a DC bias of -2V through a bias T (Agilent model 11612A, 45MHz – 26.5GHz). The AC photocurrent passes through the bias T into a 50-GHz electrical spectrum analyzer (HP model 8565E) that is internally terminated with 50 Ohms.

(a) 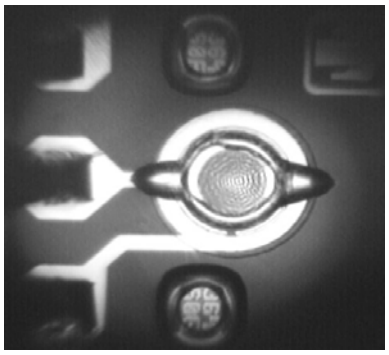 (b)

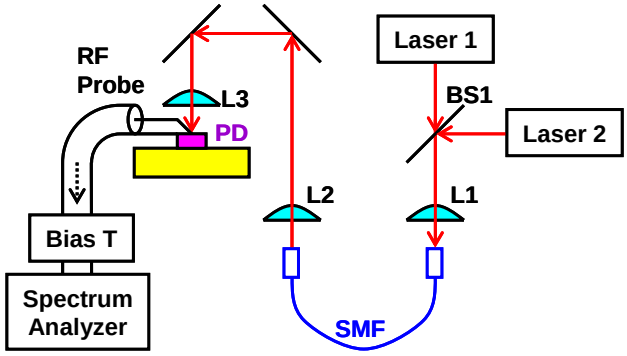


**Figure 3.8. (a) Picture of a 60-um-aperture photodiode illuminated at 850 nm and contacted with a 40-GHz coplanar probe for bandwidth measurements. (b) Schematic diagram of the bandwidth measurement setup. Two single-frequency tunable lasers are combined in a single-mode fiber to create a beatnote at the difference frequency. One laser is wavelength tuned, in approximately 0.18-GHz steps, to scan the beatnote frequency from 0 to 20 GHz while maintaining a nearly constant beatnote amplitude.**

**Error! Reference source not found.** shows the frequency response (from 0 to 20 GHz) of three neutron-irradiated photodiodes. These photodiodes (from wafer EMC8308-B) all had 2-um thick intrinsic regions. From the data in **Error! Reference source not found.**, we conclude that there was no significant change in bandwidth due to radiation at fluence levels of $1x10^{12}$, $1x10^{14}$, and $1x10^{15}$ neutrons/cm$^2$. If anything, the data in **Error! Reference source not found.** suggests the bandwidth of the photodiodes might increase from approximately 6 to 7 GHz at the highest neutron radiation levels, but we hesitate to claim a 15% increase in bandwidth given the 20% uncertainty in response amplitude.

Physically, we expect the 3-dB bandwidth of such photodiodes to be determined by the RC time constant associated with the photodiode capacitance and the load resistance. The load resistance is approximately 50 ohms (a 50-ohm coaxial cable terminated into 50 ohms inside the spectrum analyzer). We measured a 0.45pF capacitance on a 60-um-diameter-aperture photodiode, with 2-um thick intrinsic region, using an HP model 4284A Precision LCR Meter (applying 50mVpp at 10kHz, at bias voltages of 0V and -2V). Thus, we expect RC = 22.5 ps and a corresponding bandwidth $f_{3dB} = 1/(2\pi RC) = 7.1$ GHz. The measured data shown in **Error! Reference source not found.**, which includes the coaxial cable loss of approximately 0.3 dB/GHz, is consistent with the expected bandwidth of 7.1 GHz. Because the photodiode capacitance is essentially determined by the mesa area and intrinsic region thickness, it is difficult to imagine how a moderate level of defect creation due to irradiation could significantly change the photodiode capacitance. Hence, to lowest order, we expect the bandwidth to be insensitive to radiation damage.

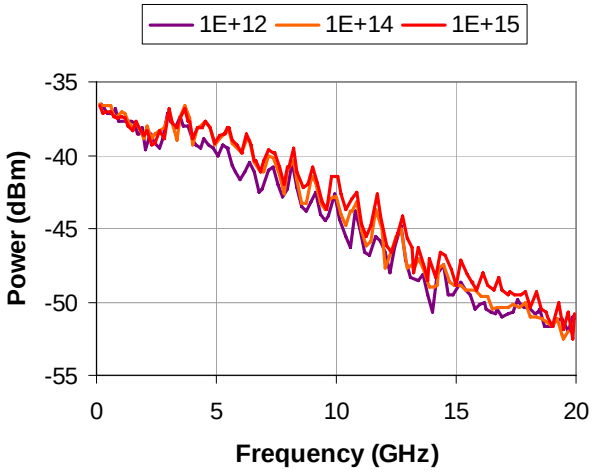


**Figure 3.9. Measured frequency response of four 60-um-aperture photodiodes subjected to different fluence levels of neutron radiation. The legend shows the fluence level in units of neutrons/cm$^2$.**

## 3.5. DLTS measurements

Deep-level transient spectroscopy (DLTS) is a measurement technique in which transient capacitance measurements are made as a function of temperature [8]. This technique can give information on the types of defects in the material and their density.

Device doping information from capacitance-voltage (CV) measurements show in Figure 3.10 that the zero-bias depletion extends essentially all the way through the intrinsic region until it hits the tail of the substrate doping near the n-type back layer. Therefore, this type of p-i-n diode is not likely to be a good candidate for useful DLTS results because there is essentially no field-dependent change of the depletion depth.

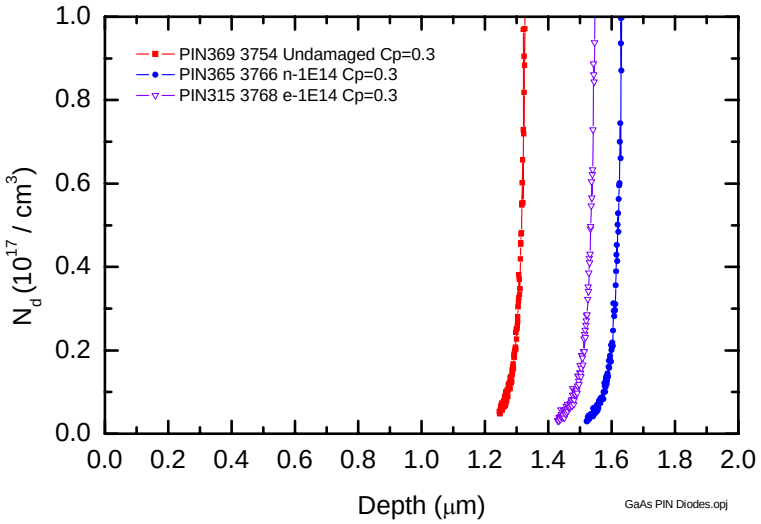


**Figure 3.10. Photodiode doping concentration vs. depth from capacitance-voltage measurements.**

As shown in Figure 3.11, DLTS measurements show some signal in the neutron damaged case and essentially no signal in the electron damaged case. This shows that the neutrons did produce defects in the device, but little information about these defects can be obtained due to the low doping and narrow width of the intrinsic region. It is not clear whether signal below 200 K is due to displacement defects or some other factor. It simply indicates that there is a temperature-induced change in the capacitance transient that is larger after neutron irradiation.

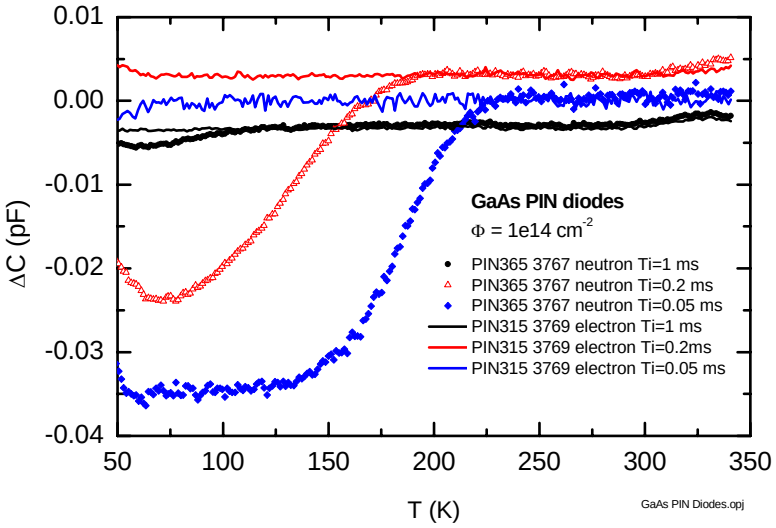


**Figure 3.11. DLTS scans of neutron and electron irradiated GaAs photodiodes.**

For comparison, Figure 3.12 shows a DLTS scan from a neutron-damaged GaAs Schottky diode [9]. This device had similar doping to the PIN diodes, but was 12 μm wide. The results show peaks in the DLTS spectrum that agree with similar data in the literature.

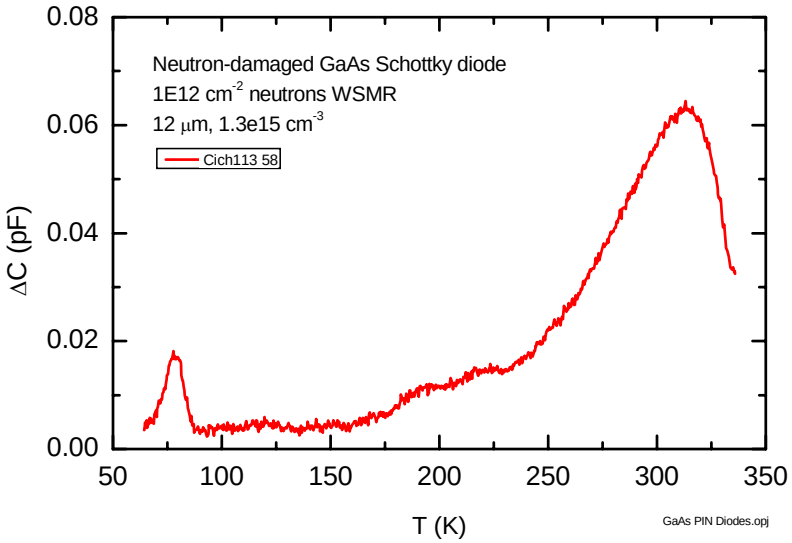


**Figure 3.12. DLTS scan of a 12 m wide Schottky diode.**

# 4. Summary

GaAs photodiodes were fabricated at Sandia's MESA facility, irradiated with neutrons and electrons at WSMR, and measurements were made to investigate changes in dark current, responsivity, and optical bandwidth. Increasing neutron fluence led to an increase in dark current at all reverse bias voltages measured. From a linear fit to the dark current vs. neutron fluence at a reverse bias of 5 V, we calculate a dark current density damage coefficient $K_{JD} = K_D/A = 1.6E\text{-}21$ A.

Responsivity measurements show that there is little detectable change up through a fluence of $10^{14}$ neutrons/cm$^2$, with only a small reduction in responsivity at the lower reverse bias values. At $10^{15}$ neutrons/cm$^2$, however, there is a significant reduction in responsivity at all reverse bias values, with the largest reduction occurring for the lowest reverse bias values. This makes sense, because at higher bias, e-h pairs are swept out of the 2-micron absorption region before they have a chance to recombine at defect sites. However, at the highest irradiation level (1E15), the responsivity is reduced for all reverse bias voltages (0 to 10V), although the responsivity is clearly much worse at 0V than at 10V, again consistent with the notion that responsivity is proportional to the number of carriers that are swept out before they have a chance to recombine at defect sites. It is worth considering this effect further. It may be possible to gain useful information on defects measuring responsivity vs. reverse bias, and considering the effects of time and temperature, analogous to DLTS measurements.

From measurements made of the optical bandwidth up to frequencies of 20 GHz, we conclude that there was no significant change in bandwidth due to radiation at fluence levels of $1x10^{12}$, $1x10^{14}$, and $1x10^{15}$ neutrons/cm$^2$. Because the photodiode capacitance is essentially determined by the mesa area and intrinsic region thickness, it is difficult to imagine how a moderate level of defect creation due to irradiation could significantly change the photodiode capacitance.

All measurements of optical device properties show no change due to electron irradiation. It is unclear why this is the case. Previously reported measurements [4] imply that there should be noticeable damage at fluence levels of $10^{15}$ electrons/cm$^2$. It is possible that there was a mistake during irradiation, and the photodiodes were irradiated with fluence levels lower than intended. Further communication with WSMR will hopefully lead to a better understanding of this result.

DLTS measurements were performed on the photodiodes which shows that the neutrons did produce defects in the device, but little information about these defects can be obtained due to the low doping and narrow width of the intrinsic region. We conclude that DLTS measurements do not produce much valuable information for these devices. However, the measurements confirm that neutron irradiation led to defect formation, and the electron irradiation did not, consistent with results from the optical measurements.

The results of the dark current, responsivity and bandwidth measurements of the GaAs photodiodes extend our knowledge of the effects of neutron irradiation on GaAs

photodiodes. The results also bring up more questions. As discussed in the introduction, previous measurements on similar vendor-bought GaAs photodiodes indicated a roughly 5% increase in responsivity at a neutron fluence of $5x10^{13}$ neutrons/cm$^2$. No increase in the responsivity was seen during these measurements. We do not know why. Further research would require looking at a large variety of photodiodes, along with designing a technique for probing the defect types and densities in the intrinsic region of the p-i-n photodiode, given that DLTS is insufficient.

# 5. References


[1] E. L. Blansett, et al., "Final Report on LDRD project 52722 Radiation Hardened Optoelectronic Components for Space-Based Applications.," Sandia National Laboratories, SAND2003-4288, Dec. 2003.

[2] V.C. Burkig, J.L. McNichols, W.S. Ginell, "Infrared Absorption in Neutron-Irradiated GaAs," J. Appl. Phys., vol. 40, pp. 3268-3273 (1969).

[3] C. Carlone, G. Bernier, E. Tannous, S.M. Khanna, W.T. Anderson, J.W. Gerdes, "The Photoluminescent Spectrum of Neutron Irradiated GaAs," IEEE Trans. Nucl. Sci., vol. 37, pp. 1718-1725 (1990).

[4] S.M. Khanna, C. Rejeb, A. Jorio, M. Parenteau, C. Carlone, J.W. Gerdes, "Electron and Neutron Radiation-Induced Order Effect in Gallium Arsenide," IEEE Trans. Nucl. Sci., vol. 40, pp. 1350-1359 (1993).

[5] O.Y. Borkovskaya, N.L. Dmitruk, V.G. Litovchenko, and O.N. Mishchuk, "Model of the Radiation-Stimulated Ordering Effect in III-V Semiconductors," Sov. Phys. Semicond., Vol. 23, pp. 129-132 (1989).

[6] J.J. Wiczer, C.E. Barnes, T.A. Fischer, L.R. Dawson, T.E. Zipperian, "AlGaAs/GaAs radiation hardened photodiodes," SPIE, vol. 506, pp. 224-230 (1984).

[7] J.J. Wiczer, T.A. Fischer, L.R. Dawson, G.C. Osbourn, T.E. Zipperian, and C.E. Barnes "Pulsed irradiation of optimized, MBE grown, AlGaAs/GaAs radiation hardened photodiodes," IEEE Trans. Nuclear Sci., vol. NS-31, pp. 1477-1482 (1984).

[8] D. K. Schroder, *Semiconductor Material and Device Characterization*, 2nd Ed., Wiley, New York (1998), pp. 290-303.

[9] Obtained by Robert Fleming from Mike Cich in 2005.

DISTRIBUTION:

| | | |
|---|---|---|
| 8 | MS1167 | E. L. Blansett, 1343 |
| 2 | MS0603 | D. K. Serkland, 1742 |
| 2 | MS1167 | E. F. Hartman, 1343 |
| 1 | MS0603 | K. M. Geib, 1742 |
| 1 | MS0603 | G. M. Peake, 1742 |
| 1 | MS0123 | D. L. Chavez |
| 1 | MS0899 | Technical Library, 9536 (electronic copy) |


Sandia National Laboratories